Real-Time qPCR as a Tool for Evaluating RNAi-Mediated Gene Silencing

Tom Van Maerken,[1] Pieter Mestdagh,[1] Sarah De Clercq,[2] Filip Pattyn,[1] Nurten Yigit,[1] Anne De Paepe,[1] Jean-Christophe Marine,[2] Frank Speleman,[1] and Jo Vandesompele[1]

[1]Center for Medical Genetics, Ghent University Hospital, Ghent, Belgium; [2]Laboratory for Molecular Cancer Biology, Flanders Interuniversity Institute for Biotechnology (VIB), Ghent, Belgium

Contact information: Jo Vandesompele, Center for Medical Genetics, Ghent University Hospital, MRB, De Pintelaan 185, 9000 Ghent, Belgium. Phone: 32-9-332-5187; Fax: 32-9-332-6549; E-mail: Joke.Vandesompele@UGent.be

Introduction

Real-time quantitative PCR (rt-qPCR) is the method of choice for accurate, sensitive, and specific quantitation of nucleic acid sequences. Applications of this technology are numerous in molecular diagnostics and virtually all fields of life sciences, including gene expression profiling, measurement of DNA copy number alterations, genotyping, mutation detection, pathogen detection, measurement of viral load, disease monitoring, and assessment of drug response. Several factors, such as careful primer design and evaluation, template preparation, implementation of a robust normalization strategy, and accurate data analysis, are essential for a successful and reliable rt-qPCR assay. In this report we describe how rt-qPCR can be implemented as a tool for monitoring silencing efficiency and assessing functional effects of RNA interference (RNAi)-mediated knockdown of *MYCN* and *TP53* genes, which are pivotal in neuroblastoma pathogenesis.

Neuroblastoma is a childhood cancer that is derived from precursor cells of the adrenosympathetic system, originating in the adrenal medulla or sympathetic ganglia. Three clinicogenetic subtypes of neuroblastoma can be discerned (Vandesompele et al. 2005), the most notorious being the subtype characterized by amplification of the *MYCN* oncogene. Amplification of *MYCN* is associated with advanced stage of disease and poor outcome, but the mechanisms by which this transcription factor exerts its oncogenic activity and confers an unfavorable prognosis are poorly understood. Another intriguing feature of neuroblastoma is the remarkably low frequency of *TP53* mutations upon diagnosis (Tweddle et al. 2003). We have previously shown that reactivation of the p53 pathway by the selective small-molecule MDM2 antagonist, nutlin-3, constitutes a promising novel approach for the treatment of neuroblastoma (Van Maerken et al. 2006).

To gain insight into the mechanism of action of *MYCN* and *TP53* genes in neuroblastoma pathogenesis, and to create a model system for future exploration of targeted therapeutics, we decided to exploit RNAi as an experimental tool for suppressing the expression of *MYCN* and *TP53*. The *MYCN* gene was transiently suppressed using several 27-mer siLentMer™* Dicer-substrate small interfering RNA (siRNA) duplexes, which are generally considered more effective at gene silencing than corresponding traditional 21-mer siRNAs (Kim et al. 2005). Stable knockdown of the *TP53* gene was achieved using lentiviral-mediated short hairpin RNA (shRNA) interference. The CFX96™ real-time PCR detection system was used as a real-time detection platform.

Methods

Cell Lines

Human neuroblastoma cell lines IMR-32 and NGP carrying wild-type p53 were grown as a monolayer in RPMI-1640 medium supplemented with antibiotics, 15% fetal calf serum, and 2 mM glutamine. Human embryonic kidney 293T cells were cultured in DMEM medium supplemented with antibiotics, 10% fetal bovine serum, and 2 mM glutamine. All cells were incubated at 37°C in a humidified atmosphere containing 5% CO_2.

siRNA Transfections and Nutlin-3 Treatment

IMR-32 cells were transfected either with 10 nM of a nonspecific control siLentMer siRNA or siLentMer siRNAs targeting *MYCN* (target sequence of siRNA 1: 5'-CGAGCTGATCCTCAAACGATGCCTTCC-3'; target sequence of siRNA 2: 5'-GACGCTGATACATAACTAAATTTGATA-3') in a 6-well plate format using 2.5 µl of siLentFect™ lipid transfection reagent per well. Silencing efficiency was assessed by rt-qPCR 48 hr after transfection. Nutlin-3 (Cayman Chemical) was dissolved in ethanol and stored at –20°C in small aliquots as a 10 mM stock solution. Cells were exposed to 0–32 µM of nutlin-3 for 24, 48, and 72 hr, with the final ethanol concentration kept constant in each experiment.

Lentiviral Vector Construction, Virus Production, and Infection

The sequence of the human *TP53* gene that was targeted using shRNA was 5'-GACTCCAGTGGTAATCTAC-3'. As a negative control, we targeted the *Trp53* gene, the murine form of p53, using the sequence: 5'-GTACTCTCCTCCCCTCAAT-3'. Pairs of complementary oligonucleotides containing these sequences

* These siLentMers were validated in Dr. Vandesompele's laboratory.

were phosphorylated, annealed, and ligated into the pSIF-H1-Puro vector (System Biosciences). The pSIF-H1-Puro vectors containing the shRNA sequences were cotransfected with two packaging plasmids (pFIV-34N and pVSV-G) (System Biosciences) into 293T cells using calcium phosphate precipitation. Viral supernatants, designated as LV-h-p53 and LV-m-p53 for lentiviruses carrying the shRNA construct against human *TP53* and murine *Trp53*, respectively, were collected and filtered through a 0.45 µm filter, and used to infect IMR-32 and NGP cells in the presence of 5 µg/ml polybrene (Sigma). Transduced cells were selected with 1 µg/ml puromycin (Sigma) for 48 hr.

Quantitation of mRNA Expression by rt-qPCR

Total RNA was extracted from cells using the RNeasy mini kit (QIAGEN), with an on-column treatment with RNase-free DNase I. After an additional RQ1 DNase treatment in solution (Promega), first-strand cDNA was synthesized from 2 µg total RNA using the iScript™ cDNA synthesis kit. Primer sequences for rt-qPCR analysis are available in the public RTPrimerDB database (http://medgen.ugent.be/rtprimerdb/) (Pattyn et al. 2006): *GAPDH* (ID #3), *SDHA* (ID #7), *UBC* (ID #8), *MYCN* (ID #180, P1; ID #3870, P2; ID #3871, P3; ID #3869, P4; ID #3868, P5), *TP53* (ID #1186, P1; ID #3872, P2), *MDM2* (ID #3499), and *BBC3* (*PUMA*) (ID #3500). rt-qPCR assay validation was performed using RTPrimerDB's in silico assay evaluation pipeline to determine specificity (BLAST), absence of secondary structure (mfold), and nucleotide polymorphisms in the primer annealing region.

In silico assay evaluation was followed by experimental evaluation of specificity and PCR efficiency using a standard curve consisting of six points of 4-fold serially diluted (64 ng down to 62.5 pg) reverse-transcribed human qPCR reference total RNA (Stratagene). (The protocol for generation of a template dilution series is available on http://medgen.ugent.be/CMGG/protocols/). Relative mRNA expression levels were determined using an optimized two-step SYBR Green I rt-qPCR assay with minor modifications (Vandesompele et al. 2002a). The PCR was run in duplicate on the CFX96 real-time PCR detection system in 15 µl reactions, containing 7.5 µl of iQ™ SYBR® Green supermix, 250 nM of each primer, and cDNA equivalent to 20 ng of total RNA. Gene expression levels and PCR efficiency, along with its standard error, were calculated using the qBase*Plus* 1.0 analysis software (http://www.biogazelle.com) (Hellemans et al. 2007), which employs a proven delta-C_T relative quantitation model with PCR efficiency correction and multiple reference gene normalization using *GAPDH, UBC,* and *SDHA* (Vandesompele et al. 2002b).

Cell Viability Assay

Cells were seeded in duplicate in 96-well plates (1 x 10^4 cells/well) and incubated for 6 hr to permit adherence to the surface. Cells were then treated with 0–32 µM nutlin-3 for 24, 48, and 72 hr. Cell viability was determined using the CellTiter-Glo luminescent cell viability assay (Promega). Three independent experiments were performed.

Results and Discussion

From Experimental Design to Analysis of an rt-qPCR Assay

Bioinformatics-based quality assessment of newly designed rt-qPCR primers can considerably improve the likelihood of obtaining specific and efficient primers. A number of quality control parameters have been integrated in our in-house developed RTPrimerDB's in silico assay evaluation pipeline (Pattyn et al. 2006) that allow for a streamlined assessment of candidate primer pairs, with automated BLAST specificity search, prediction of putative secondary structures of the amplicon, indication of which transcript variants of the gene of interest will be amplified, and search for known SNPs in the primer annealing regions. This in silico evaluation, however, does not preclude the need of experimental validation after synthesis of the primers. Ideally, experimental evaluation addresses specificity, efficiency, and dynamic range of the assay using a broad dilution series of template (Figure 1).

Purity and integrity of the RNA template are critical factors to the success of an rt-qPCR assay. Several kits are commercially available for producing clean RNA samples. Contaminants should be avoided or removed, since they can greatly influence the reverse transcription step or the actual PCR. The presence of PCR inhibitors can be assessed using a variety of methods, including the simple and fast PCR-based SPUD assay (Nolan et al. 2006a). An oligonucleotide target sequence with no homology to human DNA is spiked into human RNA samples and a water control at a known concentration. rt-qPCR quantitation of the oligonucleotide template in both the RNA samples and the (negative) water control is indicative of possible enzymatic inhibitors present in the RNA extract. For assessment of RNA integrity, electrophoresis and PCR-based methods are available (Fleige and Pfaffl 2006, Nolan et al. 2006b).

To control for inevitable experimental differences due to variables such as the amount and quality of starting material, enzymatic efficiencies, and overall cellular transcriptional activity, use of a reliable normalization strategy in which these factors are taken into account is necessary. In principle, internal reference genes offer the best way to deal with the multiple sources of confounding variables that might exist between different samples. A truly accurate normalization can be achieved only when multiple reference genes are utilized, since use of a single reference gene results in relatively large errors in a considerable proportion of the sample set (Vandesompele et al. 2002b). Because no universal set of reference genes exists, care should be taken when selecting the genes to be used for normalizing the expression levels. Different sample origins and experimental manipulations might require another set of genes to be used as reference genes. Selection and validation of reference genes can be done using the geNorm algorithm, which determines the most stable genes from a set of tested candidate reference genes in a given sample panel and calculates a normalization factor (Vandesompele et al. 2002b).

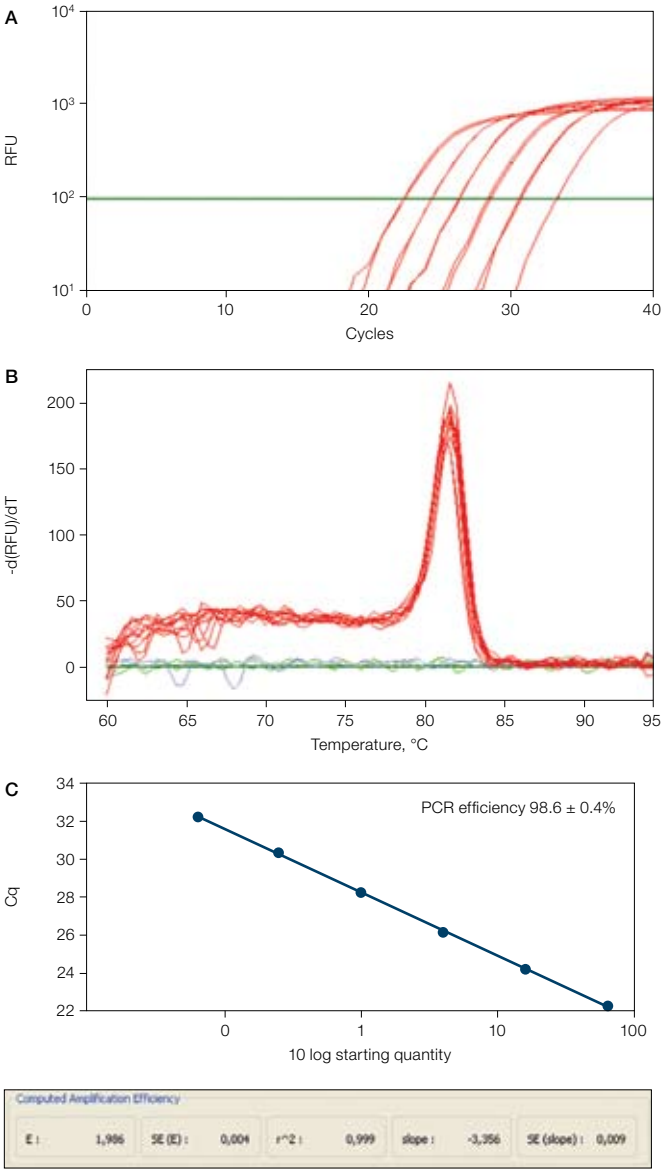

Fig. 1. Experimental validation of newly designed rt-qPCR primers. **A**, PCR efficiency and dynamic range of the rt-qPCR assay was tested using a 4-fold serial dilution of six points of reverse transcribed human qPCR reference total RNA (64 ng down to 62.5 pg) and *TP53* P2 primers; **B**, specificity of the *TP53* P2 primers was assessed by generating a melting curve of the PCR product; **C**, standard curve and PCR efficiency estimation (including the error) according to the qBase*Plus* software. Cq, quantitation cycle value.

Processing and analysis of the raw rt-qPCR data represent a multistep computational process of averaging replicate C_T values, normalization, and proper error propagation along the entire calculation track. This process might prove cumbersome and deserves equal attention as the previous steps in order to get accurate and reliable results. This final procedure has been automated and streamlined in Biogazelle's qBase*Plus* software, a dedicated program for management and analysis of rt-qPCR data (Hellemans et al. 2007).

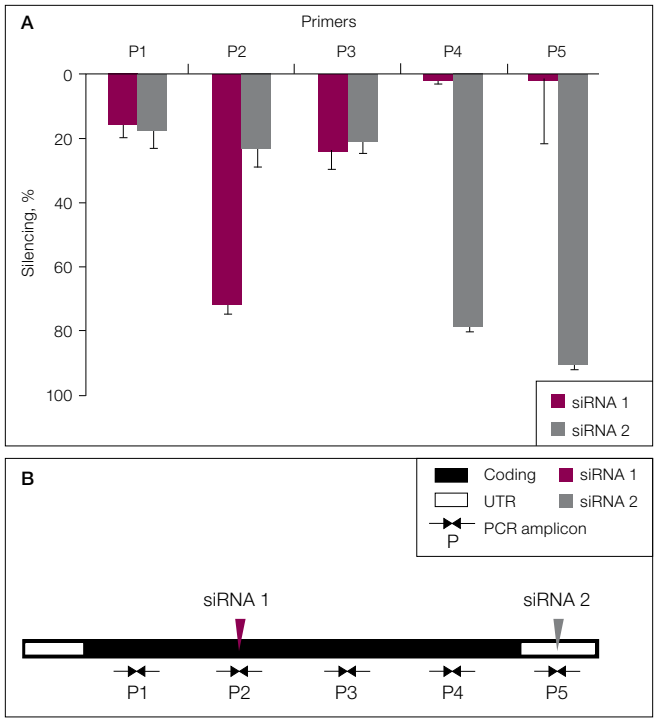

Fig. 2. Importance of primer location for rt-qPCR assessment of siRNA silencing efficiency. **A**, percentage silencing of *MYCN* gene expression measured by five different primer pairs (P1–P5) in IMR-32 cells 48 hr after transfection with anti-*MYCN* siLentMer siRNA duplexes (siRNA 1 or siRNA 2), compared to cells transfected with a nonspecific control siRNA; **B**, schematic representation of the *MYCN* mRNA structure with location of siRNA-targeted sequences and primer binding sites.

Assessment of siRNA Silencing Efficiency Using rt-qPCR in Cells Treated With Anti-*MYCN* siLentMer siRNA Duplexes

Human IMR-32 neuroblastoma cells were transfected with different anti-*MYCN* siLentMer siRNA duplexes or a nonspecific control siRNA, and the level of *MYCN* transcript was determined 48 hr posttransfection by rt-qPCR. Our results show variable levels of *MYCN* silencing with different primers (Figure 2A), which indicates the importance of primer location for evaluation of siRNA silencing efficiency, consistent with a previously published study (Shepard et al. 2005). The target mRNA sequence is cleaved by the RNA-induced silencing complex (RISC) near the center of the region complementary to the guiding siRNA (Elbashir et al. 2001). Complete nucleolytic degradation of the resulting fragments is not always guaranteed, which might result in underestimation of siRNA silencing efficiency if primers that do not span the siRNA target sequence are used for rt-qPCR (Figure 2B).

Evaluation of Silencing Efficiency and Functional Effects of Lentiviral-Mediated shRNA Knockdown of *TP53* Using rt-qPCR

To generate stable *TP53* knockdown variants of neuroblastoma cell lines that carry wild-type p53, we infected IMR-32 and NGP cells with a lentiviral vector encoding an shRNA directed specifically against the human *TP53* gene (LV-h-p53) or against the murine *Trp53* gene (LV-m-p53), as

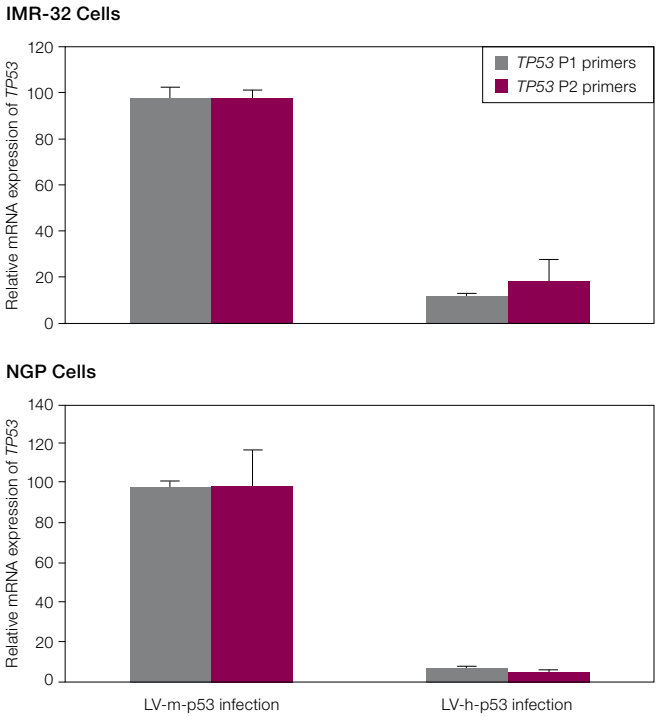

Fig. 3. Assessment of shRNA-mediated *TP53* knockdown efficiency by rt-qPCR. IMR-32 and NGP cells were infected with a lentivirus carrying an shRNA construct specific for either the human *TP53* gene (LV-h-p53) or the murine *Trp53* gene (LV-m-p53) as a control. Efficiency of *TP53* gene silencing was evaluated by rt-qPCR using two different primer pairs (*TP53* P1 and *TP53* P2). Bars indicate mRNA expression levels of *TP53*, relative to the respective LV-m-p53 infected cells; error bars depict standard error of the mean (duplicated PCR reactions for *TP53* and 3 reference genes).

a negative control. rt-qPCR analysis with two different primer pairs demonstrated that expression of *TP53* was reduced by 81–87% in IMR-32 cells infected with LV-h-p53 and by 92–94% in NGP cells infected with LV-h-p53, compared to the respective control cells infected with LV-m-p53 (Figure 3).

Functionality of the *TP53* knockdown variants was validated by rt-qPCR and analysis of cell viability after treatment with nutlin-3. This small-molecule compound selectively disrupts the interaction between p53 and its negative regulator MDM2, resulting in stabilization and accumulation of the p53 protein and activation of the p53 pathway (Vassilev et al. 2004). Lentiviral-mediated expression of shRNA against human *TP53* prevented transactivation of p53 target genes, such as *BBC3* (*PUMA) and MDM2*, by nutlin-3 (Figure 4A, B). In addition, downregulation of *TP53* transcript level by nutlin-3, a result of the ability of the p53 protein to negatively autoregulate its transcriptional expression after accumulation (Hudson et al. 1995), was abrogated in cells infected with LV-h-p53 (Figure 4C, D). At the cellular level, silencing of human *TP53* severely attenuated the cell viability response to nutlin-3 (Figure 5A, B, D, E), in contrast to control infection with LV-m-p53 (Figure 5A, C, D, F), while viability of nontransduced parental cells (Figure 5A, D) and cells infected with LV-m-p53 (Figure 5C, F) was significantly reduced when treated with increasing

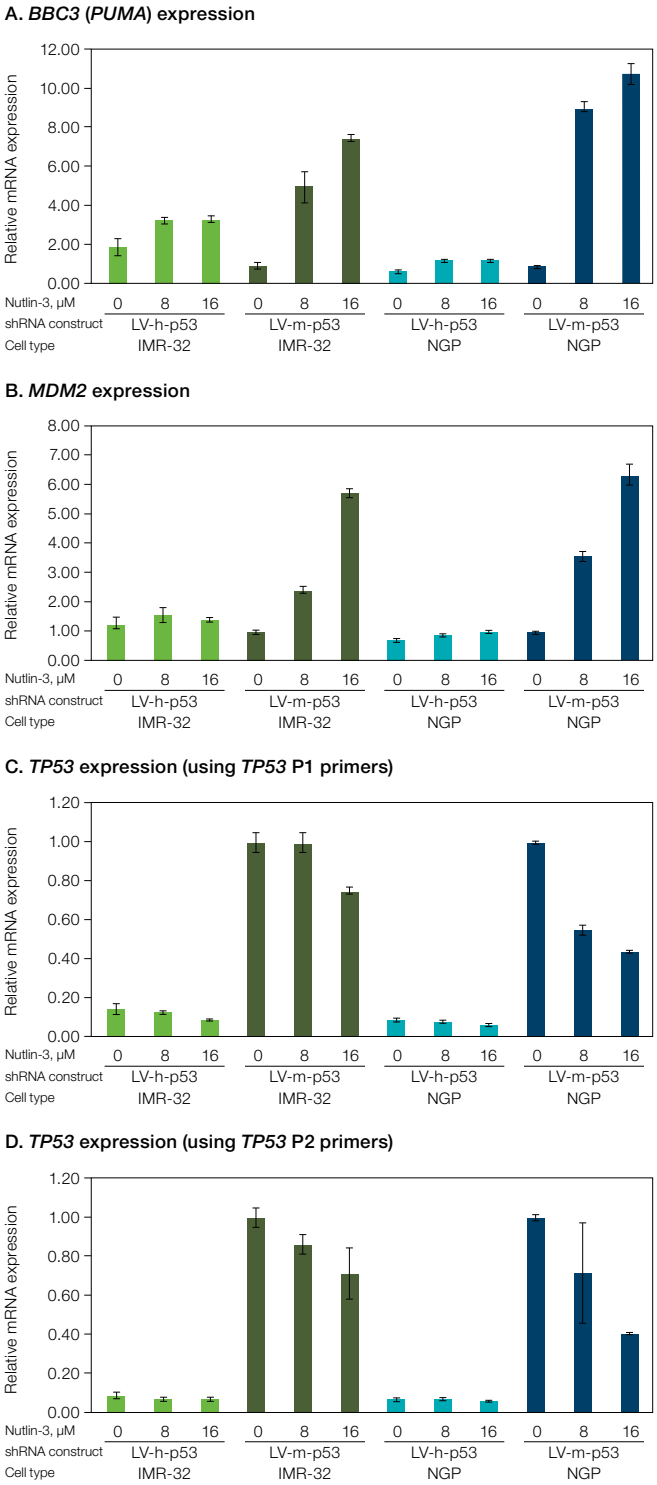

Fig. 4. Functional validation of shRNA-mediated *TP53* knockdown through rt-qPCR analysis of transcript levels of p53-regulated genes after nutlin-3 treatment. IMR-32 and NGP cells were infected with a lentiviral vector encoding an shRNA directed specifically against either the human *TP53* gene (LV-h-p53) or the murine *Trp53* gene (LV-m-p53). Cells were treated with 0, 8, or 16 μM nutlin-3 for 24 hr, and expression of *BBC3* (*PUMA*) (**A**), and *MDM2* (**B**), p53-regulated genes, and *TP53* was determined by rt-qPCR. Two different primer pairs (*TP53* P1 and *TP53* P2) were used for quantification of *TP53* transcript levels (**C**, **D**). Bars indicate mRNA expression levels relative to the respective vehicle-treated (0 μM nutlin-3) LV-m-p53 infected cells, mean of two different rt-qPCR measurements; error bars show standard error of the mean.

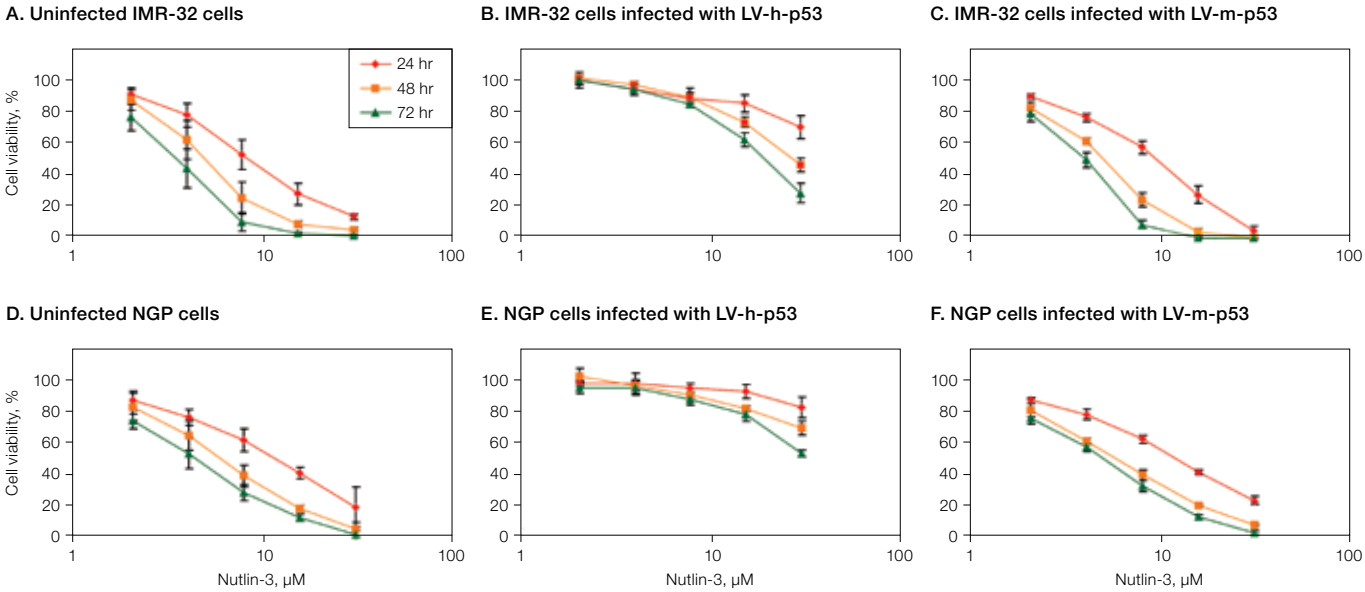

Fig. 5. Functional validation of shRNA-mediated *TP53* knockdown through cell viability analysis after treatment of IMR-32 and NGP cells with nutlin-3. Effect of nutlin-3 on viability of uninfected cells (**A**, **D**), LV-h-p53 infected cells (**B**, **E**), and LV-m-p53 infected cells (**C**, **F**). Exponentially growing cells were exposed to 0–32 µM of nutlin-3 for 24, 48, and 72 hr, and the percentage cell viability, with respect to vehicle-treated (0 µM nutlin-3) cells, was determined. Error bars indicate standard deviation of mean cell viability values of three independent experiments.

concentrations of nutlin-3. These results firmly demonstrate potent and selective impairment of p53 function in IMR-32 and NGP cells infected with a lentivirus carrying an shRNA construct against human *TP53*.

Conclusions

rt-qPCR analysis provides a convenient and reliable method for evaluating knockdown efficiency and functional effects of RNAi-mediated gene silencing, as demonstrated by the use of this tool for monitoring knockdown of *MYCN* and *TP53* genes, which are pivotal in neuroblastoma pathogenesis. Successful application of rt-qPCR requires careful attention to all of the steps in the assay workflow, including primer design and evaluation, template preparation, normalization strategy, and data analysis.

Grant Support

The Fund for Scientific Research – Flanders (FWO) grants 011F4004 (T. Van Maerken, Research Assistant), G.1.5.243.05 (J. Vandesompele) and G.0185.04; GOA grant 12051203; grants from the Belgian Foundation against Cancer (S. De Clercq), the Ghent Childhood Cancer Fund, and the Ghent University Research grant (B.O.F.) 01D31406 (P. Mestdagh, F. Pattyn).

References

Elbashir SM et al., RNA interference is mediated by 21- and 22-nucleotide RNAs, Genes Dev 15, 188–200 (2001)

Fleige S and Pfaffl MW, RNA integrity and the effect on the real-time qRT-PCR performance, Mol Aspects Med 27, 126–139 (2006)

Hellemans J et al., qBase relative quantification framework and software for management and automated analysis of real-time quantitative PCR data, Genome Biol 8, R19 (2007)

Hudson JM et al., Wild-type p53 regulates its own transcription in a cell-type specific manner, DNA Cell Biol 14, 759–766 (1995)

Kim DH et al., Synthetic dsRNA Dicer substrates enhance RNAi potency and efficacy, Nat Biotechnol 23, 222–226 (2005)

Nolan T et al., SPUD: a quantitative PCR assay for the detection of inhibitors in nucleic acid preparations, Anal Biochem 351, 308–310 (2006a)

Nolan T et al., Quantification of mRNA using real-time RT-PCR, Nat Protoc 1, 1559–1582 (2006b)

Pattyn F et al., RTPrimerDB: the real-time PCR primer and probe database, major update 2006, Nucleic Acids Res 34 (Database issue), D684–D688 (2006)

Shepard AR et al., Importance of quantitative PCR primer location for short interfering RNA efficacy determination, Anal Biochem 344, 287–288 (2005)

Tweddle DA et al., The p53 pathway and its inactivation in neuroblastoma, Cancer Lett 197, 93–98 (2003)

Vandesompele J et al., Unequivocal delineation of clinicogenetic subgroups and development of a new model for improved outcome prediction in neuroblastoma, J Clin Oncol 23, 2280–2299 (2005)

Vandesompele J et al., Elimination of primer-dimer artifacts and genomic coamplification using a two-step SYBR green I real-time RT-PCR, Anal Biochem 303, 95–98 (2002a)

Vandesompele J et al., Accurate normalization of real-time quantitative RT-PCR data by geometric averaging of multiple internal control genes, Genome Biol 3, RESEARCH0034 (2002b)

Van Maerken T et al., Small-molecule MDM2 antagonists as a new therapy concept for neuroblastoma, Cancer Res 66, 9646–9655 (2006)

Vassilev LT et al., In vivo activation of the p53 pathway by small-molecule antagonists of MDM2, Science 303, 844–848 (2004)

BIO-RAD

Bio-Rad Laboratories, Inc.

Life Science Group

Web site *www.bio-rad.com* ***USA*** *800 4BIORAD* ***Australia*** *61 02 9914 2800* ***Austria*** *01 877 89 01* ***Belgium*** *09 385 55 11* ***Brazil*** *55 21 3237 9400* ***Canada*** *905 364 3435* ***China*** *86 21 6426 0808* ***Czech Republic*** *420 241 430 532* ***Denmark*** *44 52 10 00* ***Finland*** *09 804 22 00* ***France*** *01 47 95 69 65* ***Germany*** *089 318 84 0* ***Greece*** *30 210 777 4396* ***Hong Kong*** *852 2789 3300* ***Hungary*** *36 1 455 8800* ***India*** *91 124 4029300* ***Israel*** *03 963 6050* ***Italy*** *39 02 216091* ***Japan*** *03 6361 7000* ***Korea*** *82 2 3473 4460* ***Mexico*** *52 555 488 7670* ***The Netherlands*** *0318 540666* ***New Zealand*** *0508 805 500* ***Norway*** *23 38 41 30* ***Poland*** *48 22 331 99 99* ***Portugal*** *351 21 472 7700* ***Russia*** *7 495 721 14 04* ***Singapore*** *65 6415 3188* ***South Africa*** *27 861 246 723* ***Spain*** *34 91 590 5200* ***Sweden*** *08 555 12700* ***Switzerland*** *061 717 95 55* ***Taiwan*** *886 2 2578 7189* ***United Kingdom*** *020 8328 2000*